

Sound Propagation Outdoor: Comparison between Numerical Previsions and Experimental Results

A. Farina

*Department of Industrial Engineering, University of Parma,
Via delle Scienze, I-43100 PARMA, Italy*

L.Maffei

*DETEC- University of Napoli Federico II
Pl.e Tecchio 80, I-80125 NAPOLI, Italy*

Abstract

The aim of this work is to test the accuracy of numerical previsions made following two different approaches: the first is an Image Source code, built up around the computing formulas contained in the new ISO DIS standard 9613 parts 1 and 2. The second one is a general purpose Pyramid Tracing code, called RAMSETE, that is suitable both for indoor and outdoor simulations.

The test case was chosen in an area containing all the most interesting acoustic phenomena: large distance propagation over absorbing soil, shielding by embankments and buildings, multiple reflections on reflecting facades. Only adverse atmospheric conditions were not taken into account (strong wind, inverted temperature gradient).

A new technique was employed to collect experimental data: the sound source was a directive loudspeaker, which Sound Power Levels and Directivity Balloons in Octave Bands were previously measured in free field conditions. It was fed with MLS (Maximum Length Sequence) pseudo-random continuous signal. The measurement in each point was obtained through asynchronous cross-correlation of the signal coming from a standard Sound Level Meter (recorded for convenience on a DAT tape recorder) and the original MLS sequence, through a fast-Hadamard algorithm, yielding the Impulse Response between the Source and the Receiver positions. With proper synchronous averaging of the incoming signal, a great improvement in the Signal-To-Noise Ratio was achieved, making it possible to make measurements unaffected from background noise even in highly shielded positions.

Both the experimental and previsional data were used to build graphical plots, enabling a direct comparison of the results: they show that the capability of accurately model the source directivity produce generally a better estimate using the pyramid tracing algorithm, but the shielding effects are more accurately modeled by the ISO9613 code.

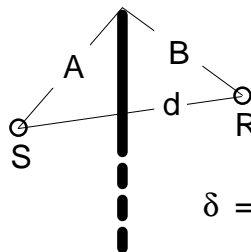
1. Pyramid Tracing model

The pyramid tracing program here employed was already introduced elsewhere by one of the authors (Farina [1,2]). It must be noted, however, that in outdoor propagation there is not any reverberant queue to be “corrected”, and that a large number of pyramids can be used with very little computation times, as most of them are “lost” after a little number of reflections: so there are not, in general, “missing” image sources as it happens in indoor cases.

The algorithm requires however proper extensions to take into account shielding effects and excess attenuation, that are discussed here. The evaluation of the sound energy diffracted from the free edges of a screen is made using the well-known Kurze-Anderson[3] formula:

$$L_{\text{diff}} = L_{\text{dir}} - 5 - 20 \cdot \lg \left(\frac{\sqrt{2 \cdot \pi \cdot |N|}}{\tanh \sqrt{2 \cdot \pi \cdot |N|}} \right) \quad (1)$$

in which L_{dir} is the Direct Level, that should arrive to the receiver if the screen were not in place, and N is the Fresnel number, given as:



$$N = \frac{2}{\lambda} \cdot \delta = \frac{2 \cdot f}{c} \cdot \delta \quad (2)$$

$$\delta = A + B - d$$

When a surface is declared “obstructing” in the input data file, a check is made for finding its free edges. For each free edge found, an energy contribution to the receiver is calculated with the above formulas, plus the energy passing “through” the panel (reduced of its sound reduction index): this happens both for the direct wave, both for the reflected ones. However, the code does not check for double diffractions, as shown in fig. 1 (no diffraction is considered at the left side of the screen):

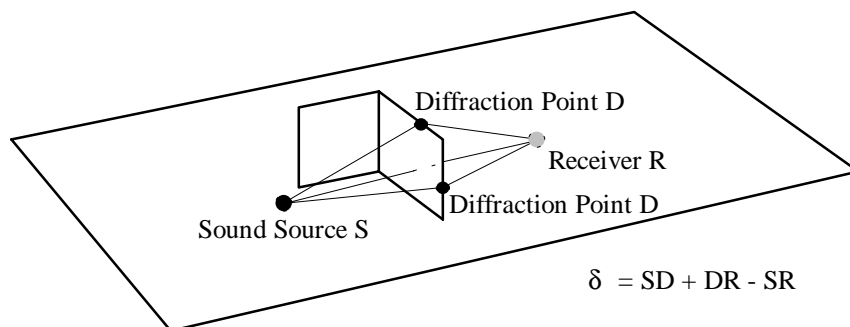


Figure 1 - Free Edge diffraction plus energy passing through the panel

The other great problem in outdoor propagation is the excess attenuation. It is known that it results from many different phenomena: air absorption, grazing incidence over the absorbing soil, interference between the direct field and the reflected one over reflecting soil, ray curvature due to wind or temperature gradients.

Only the first effect (air absorption) is taken into account in Ramsete, and only with a simplified formulation: in fact, Sound Energy Density W is reduced during the propagation by multiplying for an exponential extinction term:

$$W = W_0 \cdot e^{-\gamma \cdot x} \quad (3)$$

and the frequency-dependent extinction coefficient γ is computed taking into account only the percent relative humidity of the air $\phi\%$ (0-100%):

$$\gamma = \frac{1.7 \cdot 10^{-8} \cdot f^2}{\phi\%} \quad (4)$$

All the input data must be introduced in the octave bands from 20 Hz to 16 kHz: Power Levels and Directivity Balloons of the sources, absorption coefficients and sound reduction indexes of surfaces. The computations are made for each octave band, and then the overall Lin and A-weighted Sound Pressure Level are post-computed.

2. Image Sources code following ISO 9613

The new ISO-DIS 9613 (parts 1 and 2) standard contains a detailed method for computing the sound propagation outdoors, taking into account also the effects caused by the propagation over soil with varying properties, shielding both from thin and thick obstacles, effects of vegetation layers, excess attenuation. In particular, the air absorption is treated with great detail: the whole part 1 of the standard covers this only point.

The sound level at the receiving point is calculated with the following formula (ISO 9613 part 2):

$$L_{\text{rec}} = L_w + 10 \cdot \lg\left(\frac{Q}{4 \cdot \pi \cdot d^2}\right) - A_{\text{air}} - A_{\text{ground}} - A_{\text{screen}} - A_{\text{refl}} - A_{\text{misc}} \quad (5)$$

The (quite complex) expressions for the attenuation terms in eqn (5) are not reported here, as they are part of an ISO standard. However, some detail is needed to understand the implementation of that equation in an automated computing code.

Each sound source is introduced simply by its Cartesian coordinates, followed by the Sound Power Levels in octave bands from 63 Hz to 8 kHz and Directivities in dB ($= 10 \cdot \log Q$).

The soil is divided in homogeneous quadrilateral areas, described by their X-Y coordinates (only flat land areas are considered for now): the soil can be only classified as “hard” , “soft” or “very soft”.

Vertical reflecting surfaces (walls, screens, etc.) are introduced by the coordinates of their upper edge: these surfaces are characterised by absorption coefficients in octave bands.

It is possible also to introduce dense foliage volumes, as quadrilateral areas with a fixed height. By the same technique it is possible to introduce areas with partial building coverage or other partially obstructed volumes.

The computation algorithm automatically identifies the soil area covered by the rays, and identifies any potentially diffracting edge (horizontal or vertical). A check is made also for multiple diffractions, discarding non-relevant edges by a minimum-distance technique, as shown from figure 2:

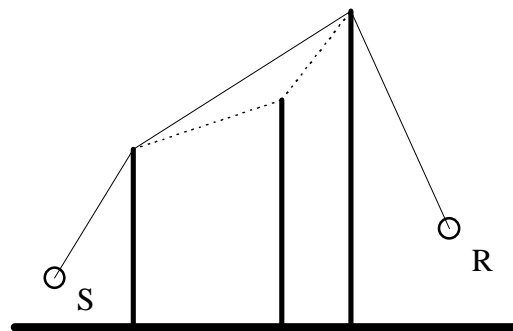


Figure 2 - Determination of the diffracted path with multiple screens

The reflections over vertical surfaces (giving “negative” attenuation A_{refl}) are taken into account generating the image source for each vertical surface, and checking it for visibility “through” the area of the surface itself. A further check is made to discard image sources shielded by other vertical surfaces, but in this case no further diffraction computation is made, and the energy that comes from a reflection followed by a diffraction is completely neglected.

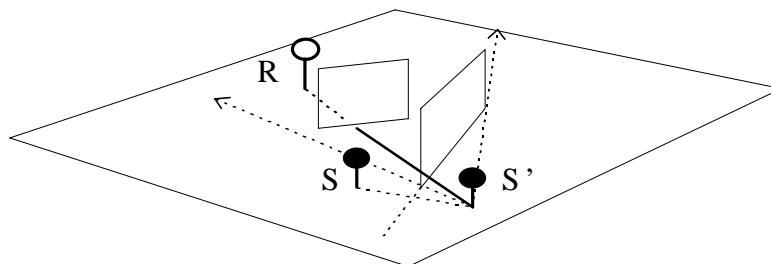


Figure 3 - check of visibility of an Image Source

3. Experimental Measurements

An innovative measuring technique was used to collect experimental data with little background noise contamination. It is based on the mathematical properties of the MLS (Maximum Length Sequence) excitation signal, as suggested by CHU [4].

A small loudspeaker is fed, through a battery operated power amplifier, with the steady MLS signal produced by a MLSSA A/D board installed in a portable computer. The measuring device is a sound level meter, with a digital DAT recorder connected to its calibrated AC output; this way no connection exist between the signal generator and the recording device.

After the recordings have been made in all the measuring points, the DAT recorder output is connected with the input of the MLSSA board, and through asynchronous cross correlation of the recorded signal with the original MLS, the impulse response between source and receiver is recovered. The recordings are calibrated, so “true” SPL values can be measured in octave bands with the post processing tools of the MLSSA software. However a check on the overall SPL shown on the S.L.M. display was always successfully made, showing maximum difference of 0.3 dB.

The MLS measurements are inherently immune from background noise, because the cross-correlation process gives a S/N improvement of nearly 30 dB against traditional “real-time” measurements. Furthermore, a synchronous averaging of 16 consecutive samples was performed, giving another 12 dB improvement of the S/N ratio. With this technique, any background contamination was avoided at frequencies of 125 Hz and up. At the lower frequency bands (31.5 and 63 Hz), some background noise was visible in the points located vary far from the source, but this was not caused from the MLS measuring system, but from the sound source, that was very inefficient at these low frequencies.

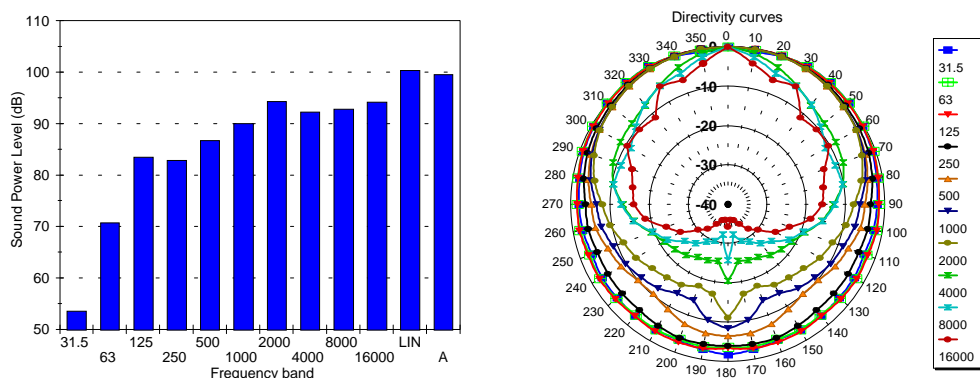


Figure 4 - Power Levels and Directivity of the Sound Source

Figure 4 shows the source characteristics as Sound Power Spectrum and as Directivity curves. As the source is perfectly axisimmetrical, just one plane of directivity was needed to completely characterise its directivity balloon.

3.1 Test Case

The measurements were performed at the University Campus of Parma, in an empty car park and between the buildings of the Faculty of Engineering. In figure 5 (actually it is a printout of the Ramsete Cad model) it is possible to see the source position (labelled “A”) and the 16 microphone positions, placed on a straight line and spaced 10m each other. The source axis was pointed towards the buildings, being parallel to the measurement line.

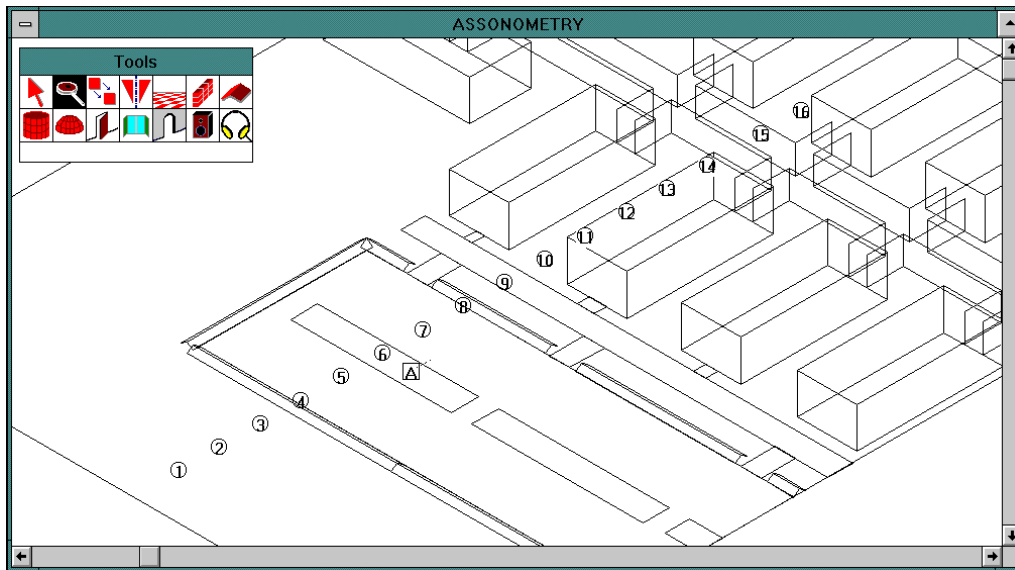


Figure 5 - 3D view of the geometry studied

This test case involves propagation on 2 different kinds of ground (hard asphalt and grass), with embankments having an height of 1m and with buildings 10m and 7m tall. The facades of these buildings are continuous crystal. The source height was 1m, and the microphones were placed at 1.3m over the soil.

In each measurement position a digital recording of 60s of MLS signal was made. Furthermore, another 60s recording without the signal was performed, to verify the background noise level. As the overall sound power level of the loudspeaker was limited (100 dB), in many points the signal felled under the background noise, but it was still possible to measure it thanks to the MLS properties.

4. Comparative results

The experimental results are presented together with the numerical simulations, to make it easy to compare them and to exploit the discrepancies.

Looking at figure 6, it is clear that the Ramsete code gives better results near the source, while the ISO-DIS 9613 is more accurate in the points at larger distance and very shielded from the buildings. This result is quite obvious, as Ramsete manages properly multiple reflections and consider the effective

directivity balloon for each of them, but does not include any evaluation of many excess attenuation effects. Furthermore, it seems that ISO-DIS 9613 is more accurate in the evaluation of the shielding effect caused by the buildings, that is overestimated by Ramsete.

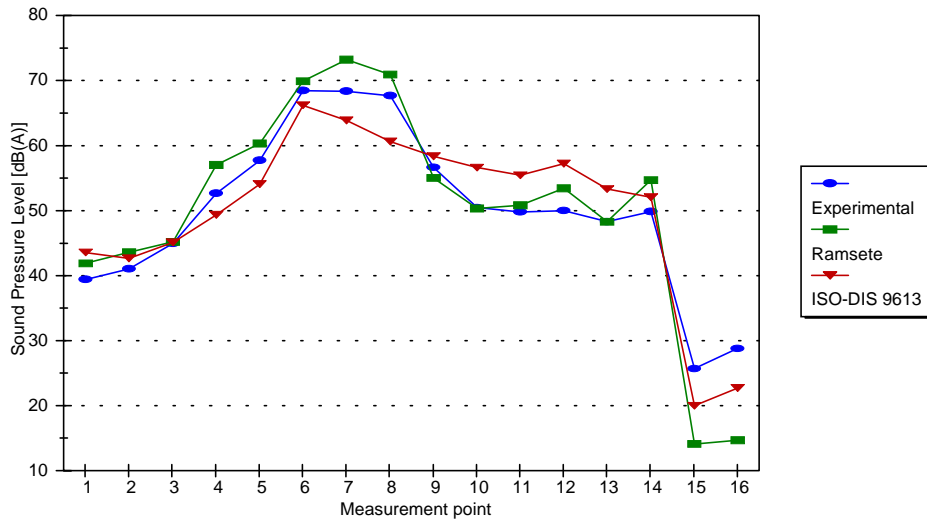


Figure 6 - Comparison of the results in dB(A)

Other interesting things come out observing the spectra in some particular points:

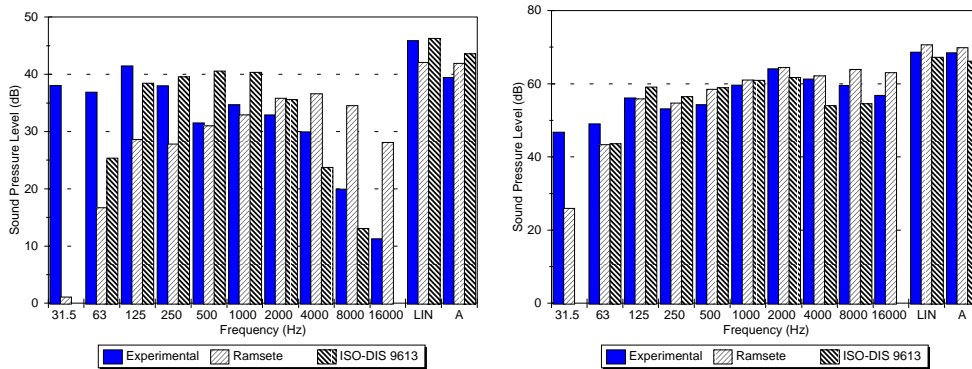


Figure 7 - Spectra at point # 1 (left) and # 6 (right)

It can be observed that in point 1 (behind the source, and partially shielded), the three spectra are quite different: the experimental one exhibits large background noise contamination in the low frequency bands, while Ramsete overestimates the high frequency bands level of more than 10 dB. It is evident at this point that the air absorption formula (eqn. 4) is not realistic enough to take into account what it happens on a soft grass soil; this instead seems well modeled by the ISO-DIS 9613 code.

But if we look at what happens in point 6 (that is the nearest to the sound source), we find that here the three spectra are very similar: obviously at this

little distance the excess attenuation terms are not very important, and the spectra modification is mainly governed by the source directivity.

As Ramsete does not compute just the sound pressure levels, but records the impulse response between source and receiver, it is possible to compare it with the experimental one, as shown in fig. 7: it can be seen how the principal specular reflections are properly modelled.

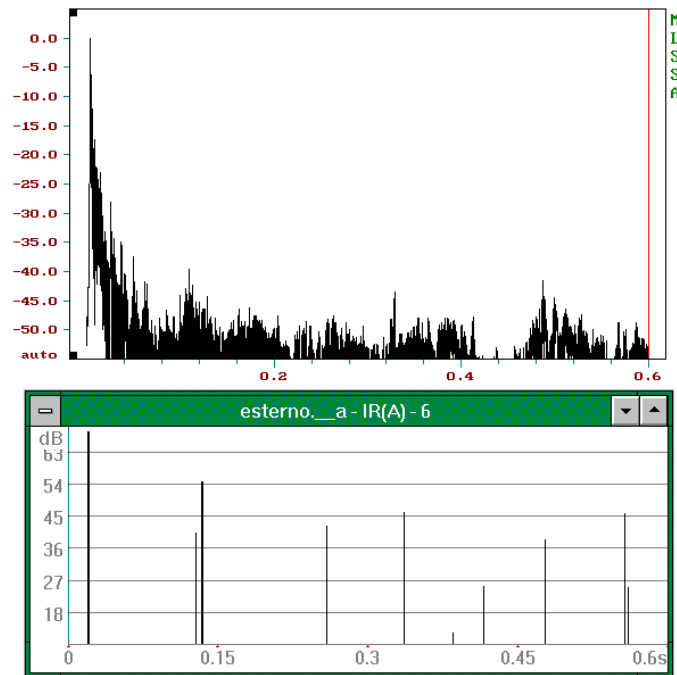


Figure 8 - Comparison between experimental and numerical I.R. - point # 6

5. Conclusions

The results show that actually none of the two numerical model employed is always accurate, each having some benefits and some defects. In the prosecution of this work the advanced capabilities of managing excess attenuation contained in the ISO-DIS 9613 shall therefore be added to the pyramid tracing code.

References

- [1] Farina, A. RAMSETE - a new Pyramid Tracer for medium and large scale acoustic problems, *Proc. of Euro-Noise 95*, Lyon, France 21-23 march 1995.
- [2] Farina, A. Pyramid Tracing vs. Ray Tracing for the Simulation of Sound Propagation in Large Rooms, in COMACO95, *Proc. of Int. Conf. on Computational Acoustics and its Environmental Applications*, Southampton, England, 1995, Computational Mechanics Publications, Southampton 1995.
- [3] Kurze, U.J. Noise Reduction by Barriers, *Journ. of Ac. Soc. America*, vol. 55 (1974), pp. 504-518.
- [4] Chu, W.T. Impulse Response and Reverberation Decay Measurements Made by Using a Periodic Pseudorandom Sequence", *Applied Acoustics*, vol. 29 (1990), pp. 193-205.